Draft version January 24, 2022
Typeset using LaTeX **twocolumn** style in AASTeX63

Investigating the Dominant Environmental Quenching Process in UVCANDELS/COSMOS Groups

Maxwell Kuschel,[1] Claudia Scarlata,[1] Vihang Mehta,[2] Rogier Windhorst,[3] and The UVCANDELS Team[2]

[1] *University of Minnesota, Minneapolis, MN, USA*
[2] *IPAC/Caltech, Pasadena, CA, USA*
[3] *Arizona State University, Tempe, AZ, USA*

(Dated: January 24, 2022)

ABSTRACT

We explore how the fraction of quenched galaxies changes in groups of galaxies with respect to the distance to the center of the group, redshift, and mass using logistic regression. With the zCOSMOS 20k Group Catalog and the new spectral energy distribution (SED) fits from UVCANDELS, we analyse 53 galaxies in 20 groups across a redshift range of $0.2 < z < 0.8$. Utilizing model spectra from UVCANDELS, we were able to construct a UVJ diagram to differentiate quenched and star-forming galaxies. We separated our analysis into two redshift bins, $0.2 \leq z < 0.45$ and $0.45 \leq z < 0.8$. We find that as we go down in redshift the probability of group galaxies being quenched increases, from $0.66^{+0.11}_{-0.08}$ at $z = 0.8$ to $0.75^{+0.14}_{-0.08}$ at $z = 0.2$, deviating from the field galaxies. The number of galaxies that are quenched also increases as we go towards the center of groups in the lowest redshift bin, from $0.40^{+0.25}_{-0.34}$ at the outskirts to $0.86^{+0.09}_{-0.11}$ in the center, again at values higher than field galaxies. These results suggest that, in general, massive galaxies in groups require several billion years to undergo significant environmental quenching, suggesting the dominant environmental quenching process in these groups is a slow process, such as strangulation or rapid-then-delayed.

1. INTRODUCTION

Star formation in a galaxy requires the cooling of gas that eventually collapses and forms stars (Jeans & Darwin (1902)). As a galaxy evolves through star formation, it consumes its cold gas content, eventually leading to the cessation of the star formation if the cold gas reservoir is not replenished. Galaxies are both observed and predicted to be hosted in halos containing large amounts of warm/hot gas that slowly fuel star formation over time (Lilly et al. (2013), Ford et al. (2016), Werk et al. (2016)). Both in the local universe, and out to redshifts ≈2 galaxies are observed to obey a bimodal distribution in their level of star-formation (Brammer et al. (2011), Muzzin et al. (2013), Peng et al. (2010)). Most galaxies are forming stars at all redshifts, the extent to which depends both on a galaxy stellar mass and its redshift (Speagle et al. (2014)). At all times, however, there exists a population of galaxies in which no new stars are being formed, having ended all significant star-formation at earlier times. These galaxies are typically referred to as quenched, quiescent, or passive galaxies. Various mechanisms have been proposed to explain why a galaxy stops forming stars. These mechanisms could be internal to the galaxies themselves (Martig et al. (2009), He et al. (2019), Murray et al. (2011)) or be the result of interactions between galaxies and the environment in which they reside.

In this paper we investigate the role that the group environment plays in determining a galaxy's probability of being quenched. In what follows, we will refer to "environmental quenching" as the ensemble of physical processes that affect the star-formation rate in galaxies, and are a consequence of the fact that a galaxy resides in a subhalo of a more massive halo. We will also work to separate this effect from the quiescent population due to internal processes driving quenching, known as "mass quenching", as it has been shown to be the dominant driver of quenching overall (REF).

Star-formation is regulated by the interactions (gravitational and/or hydrodynamic) between the galaxies' gas and the dark matter halo and/or gas content of the host halo. Tidal- and ram-pressure stripping are very efficient mechanisms, particularly in the cluster environment (McPartland et al. (2016)). Ram-pressure stripping results from the relative motion of satellites inside a gas rich halo (Gunn & Gott (1972)), while tidal stripping is a consequence of varying tidal forces acting on a satellite as it moves in the gravitational potential of the halo (Moore et al. (1996)). These mechanisms are particularly efficient in massive, cluster-size, halos and

on low-density galaxies, but are also observed in smaller group-size halos (Jian et al. (2017), Larson (1972)).

Broadly speaking, two main paths are possible for the quenching of star formation in satellites, which are characterized by the associated time-scales. Ram-pressure stripping can influence star-formation by directly removing the galaxy's cold gas (i.e., the interstellar medium) and stripping the outer, lower-density material (Gunn & Gott (1972)). Ram-pressure stripping is an example of a rapid quenching process, and quenching the galaxy in a few million years. Strangulation occurs when only the outer material is stripped, leaving the ISM untouched to continue forming stars for several billion years (Larson et al. (1980)). Because the ISM is left this process is much slower than Ram-Pressure Stripping, quenching on timescales of ~ 3 Gyr (Kawata & Mulchaey (2008)).

We attempt to disentangle the relative importance of fast and slow quenching mechanisms by investigating the probability that a galaxy is quenched as a function of a measurement of how long a galaxy has been in a group/cluster. Statistically, the amount of time a galaxy has spent in a group/cluster after falling in is related to its distance from the group's center (Gao et al. (2004), Taranu et al. (2014)).

In this paper we investigate the role of fast versus slow quenching mechanisms in groups by studying how the probability that a galaxy is quenched depends on its distance from the group's center. We focus on galaxy groups identified in the COSMOS field (Section 2), and use the stellar population properties derived using the new UVCANDELS dataset of Wang et al in prep. (Section 2). Our results are presented in Section 4 and discussed in Section 5. Throughout the paper, we assume a standard ΛCDM cosmology with parameters $H_0 = 68.8$km/s/Mpc, $\Omega_M = 0.315$ and $\Omega_\Lambda = 0.685$, all magnitudes are expressed in the AB system (Oke (1974)), and where applicable we use the Chabrier IMF (Chabrier (2003)).

2. THE DATA

In this work we study the fraction of quenched galaxies in groups and in the field. For this analysis we start from the galaxy groups identified in the zCOSMOS 20k Group Catalog of Knobel et al. (2012, hereafter K12, Section 2.2). We derive new estimate of the galaxy physical properties (mass, sfr, and rest frame bandpass strengths) using data from the UVCANDELS program (Mehta et al. in prep, Section 2.1).

2.1. *UVCANDELS Catalog*

The CANDELS/COSMOS field is one of the four target fields of the UVCANDELS program, that has recently added F275W and F435W deep imaging observations to existing datasets on these fields. The addition of the observed UV is particularly important for this analysis, as it allows more accurate estimates of star-formation-rates (SFR), dust extinction and age of the stellar population.

For all galaxies in the UVCANDELS fields we have re-derived their physical properties by fitting their spectral energy distributions (SEDs) obtained adding the new F275W and F435W fluxes to existing data on the fields. Existing photometry on the COSMOS field includes the *HST/ACS* F606W and F814W bands as well as the *HST/WFC3* F125W and F160W bands available from Nayyeri et al. (2017). We also include the photometry for *CFHT/MegaPrime* $u^\star$, $g^\star$, $r^\star$, $i^\star$ and $z^\star$, the *Subaru/SuprimeCam* B, g^+, V, r^+, i^+ and z^+, *VLT/VISTA* Y, J, H and K, *Mayall/NEWFIRM* $J1$, $J2$, $J3$, $H1$, $H2$, and K as well as *Spitzer/IRAC* ch. 1, 2, 3 and 4 bands that are also available as part of the Nayyeri et al. (2017) catalog. We use photometric redshifts that have been computed with the inclusion of the new UVCANDELS F275W and F435W photometry (REF?). In order to avoid issues when fitting, we impose an error floor of 0.02 mag on all photometry.

The stellar physical properties used for the analysis presented in this work are computed using CIGALE (Code Investigating GALaxy Emission; Boquien et al. 2019; Burgarella et al. 2005; Noll et al. 2009). The full description of the SED fitting procedure for the UVCANDELS catalog will be presented in a future publication (Mehta et al. in prep.). Briefly, the galaxy physical properties are estimated assuming a delayed exponential form for the star-formation history (SFH), with the possibility of a 10 Myr burst with an exponential e-folding time of 50 Myr and a Chabrier (2003) initial mass function. The age, e-folding time (τ) of the delayed exponential part of the SFH, and metallicity of the stellar population are varied as free parameters. We assume a modified Charlot & Fall (2000) dust model included within CIGALE to fit the V-band attenuation due to dust.

2.2. *Selection of group and field galaxy samples*

In this work, we rely on the zCOSMOS 20k Group Catalog presented in K12. K12 use accurate spectroscopic redshifts from the zCOSMOS catalog of Lilly et al. (2009) to identify group galaxies using two common group-finding algorithms, Friends-of-Friends and the Voronoi-Delaunay Method (Knobel et al. 2009). These algorithms were calibrated using simulated mock galaxy catalogs extracted from the Millenium I Dark Matter N-Body simulation (Springel et al. (2005)) by

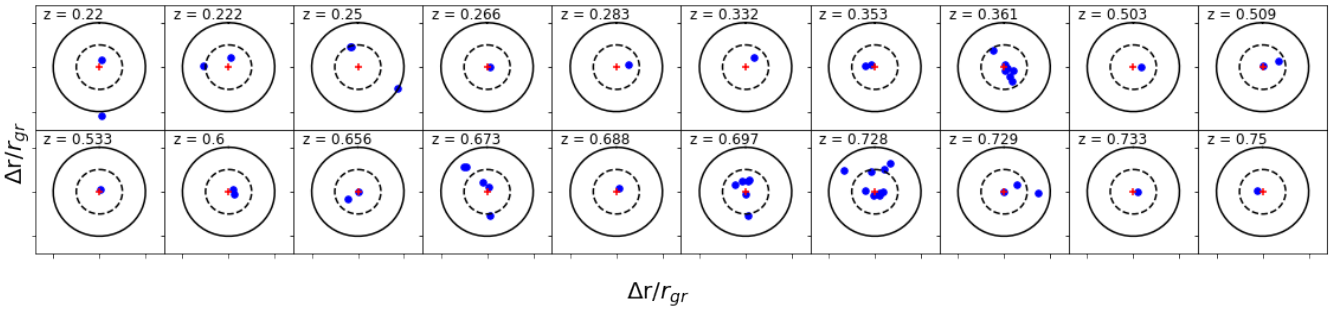

Figure 1. Stamps of each group with the radius from K12 plotted in black. Each stamp is normalized by r_{gr}, the radius of the group, to allow for easier comparisons. The black dashed line is positioned at 0.5 $\Delta r/r_{gr}$ as a visual aid. Only galaxies that make the luminosity and mass cuts described in Section 2 are plotted. The group centers are ploted with a red plus sign.

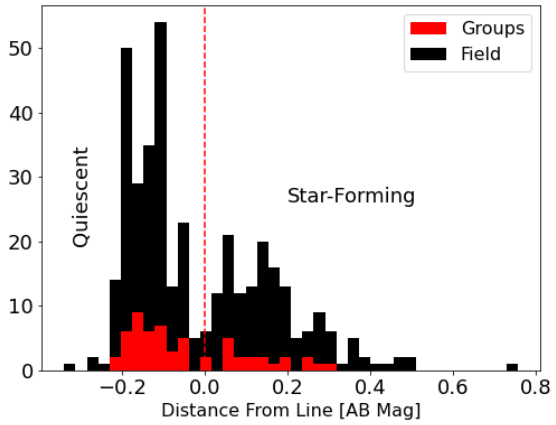

Figure 2. Histogram of distances to the UVJ cut, in AB Mag. The vertical dashed line indicates the UVJ cut that was used, created through an iterative process. First we adjusted the slope of the line to display the highest degree of bimodality. Then we adjusted the intercept of the line so it would lie between the two peaks of the distribution. Negative values are quiescent, positive values are star-forming. Distances were only calculated for galaxies with $U-V > 1.3$.

(Kitzbichler & White (2007)). The mock catalogs were used to fine-tune the parameters of the group identification algorithms in order to return a completeness and purity of groups (with more than 3 members) of $\gtrsim 80\%$.

After obtaining a catalog of groups K12 went through a process of finding what they call 'fudge' values to describe groups and their members. Among these determined values was the projected radius of the group, taken to be the effective radius of the group's dark matter halo. They determined these radii by binning their mock catalogs by redshift, richness, and apparent projected group radius. They then found the average projected radius for each bin. This defined a 2D surface which they could then use to estimate the real groups' radii based off of their richness, redshift, and apparent projected size of the group. While this fudge radius is not the same as the true effective radius of the halo it is its typical value and has been shown in K12 to be better than using the rms, detailed in K12 Section 5.1. Therefore, we utilize the fudge radius as the radius of the group, keeping in mind this is only an estimation of the true radius of the halo.

Here we limit the analysis to 60 groups in the area covered by the UVCANDELS data in the COSMOS field. In order for a group to be considered "covered" in the UVCANDELS area, we require that the projected size of the group, taken to be 1.5x the group radius, falls within the UVCANDELS/COSMOS field. The K12 catalog also reports a probability for a galaxy to belong to its host group, computed from the redshift difference and projected distance between the galaxy and the group center. In the analysis below, we only include galaxies that have a probability ≥ 0.8. K12 also defined the probability of a group existing, GRP2, based off of whether the group was found using both group finding algorithms they employed. We only considered groups with GRP2 = 1.0 to ensure we were only looking at groups that confidently exist. We only consider groups with at least 3 spectroscopic members, to ensure the high values of completeness and purity described in K12. Richness was also given an upper inclusive limit of 25 members, to avoid contaminating our group sample with cluster galaxies. Richness was only calculated using group members that had a probability of ≥ 0.8 of being in the group. With these cuts we are left with our 22 groups across our redshift range.

In order to extract the sample of galaxies used in the analysis below, we apply criteria based on redshift, magnitude, and stellar mass. Ideally, a volume limited sample constructed by selecting all galaxies brighter than a rest-frame luminosity would ensure that we are comparing the same objects at all redshifts (e.g., Presotto

et al. 2012). A typical choice in the literature is to use the evolution-corrected $B-$band luminosity. The K12 group catalogs inherits the selection function of the parent zCOSMOS catalog that includes all galaxies with I_{F814W} magnitude brighter than 22.5. The I_{F814W} filter samples the rest-frame $B-$band at $z \sim 0.8$, so that at this redshift the completeness of a $B-$band selected catalog does not depend on galaxy colors. The resulting catalog, however, would still be affected by strong mass-dependent biases, as old galaxies of a given stellar mass would preferentially be excluded compared to young galaxies of the same stellar mass, given their higher M/L ratio. Additionally, at redshifts higher(lower) than 0.8, a pure rest-frame $B-$band luminosity selection would preferentially exclude red(blue) galaxies, introducing additional mass-dependent biases in the final sample. In order to limit these effects, we follow Presotto et al. (2012) and define a luminosity and mass limited sample of group (and field) galaxies as follows.

First, we use an evolving $B-$band luminosity cut assuming the luminosity evolution from Zucca et al. (2009) where $M^*_{Bev} = -20.3 - 5\log(h_{70}) - 1.1z$. This corresponded to a cutoff in $B-$band absolute magnitude of $M_{B,cut-off} = M^*_{Bev} + 0.8$ which we have used in our sample. The mass cut they derived followed the same approach of Iovino et al. (2010). This resulted in a mass cut of $\log(M_{cutoff}/M_\odot) = 10.56$. More details on the methods used to derive the mass and luminosity cuts can be found in Presotto et al. (2012) Section 5.1. The final volume mass-limited sample of group galaxies include 19 galaxies in 8 groups in the $0.2 \leq z < 0.45$ redshift range and 34 galaxies in 12 groups in the $0.45 \leq z < 0.8$ redshift range.

The comparison sample of field galaxies was selected from the UVCANDELS catalog, applying the same redshift, magnitude and mass cut as for the group galaxy sample. These cuts result in 182 and 155 field galaxies in the low and high redshift range, respectively.

3. ANALYSIS

3.1. *Selection of quenched galaxies*

The criterion used to separate quenched from star-forming galaxies can influence the quenched fraction, particularly at the high mass end ($\gtrsim 10^{10.5}$M$_\odot$). Donnari et al. (2021) demonstrated that there is overall agreement among various definitions below this threshold. For larger stellar masses, however, different criteria for the identification of passive galaxies result in quenched fraction that can vary between 50-60% to 70-80% or 90-100%, depending on whether galaxies are centrals or satellites. We have tested varying methods for determining quiescence, detailed in Section 5, and find that the methods we use does not change the trends we observe.

Here we proceed to use a rest-frame color selection based on the position of galaxies in the rest frame $U-V$ vs rest frame $V-J$ diagram (e.g., hereafter UVJ diagram Williams et al. 2009; Martis et al. 2016; Whitaker et al. 2015). We will follow the recommendations of Donnari et al. (2021) and limit the comparison with works using similar approaches as ours.

Figure 3 shows the UVJ diagram for galaxies both in groups and in the field. The rest–frame colors were computed from the best fit models of the UVCANDELS data derived with CIGALE (Mehta et al. in prep) using the Johnson U, V, and J bandpasses. Galaxies are color-coded according to their sSFR, as shown in the color-bar on the right hand side of the figure. Quiescent galaxies lie in the cloud on the top right of the distribution, marked by a generally lower sSFR that is commonly associated with quiescence (Williams et al. (2009); Whitaker et al. (2012); Speagle et al. (2014)). To determine the exact cut to separate the quiescent galaxies we took advantage of the bi-modality of the joint distribution of colors, following the method introduced by Williams et al. (2009). Specifically, to all galaxies with $(U-V) > 1.3$[1] we consider a first diagonal cut that visually separates the populations of star-forming and quenched galaxies. We consider the field galaxy population, as the large number of galaxies makes the bi-modality of the color distribution more prominent. For each galaxy, we then computed the normal distance (in the UVJ plane) to the diagonal dividing line and plot the histogram of the distances in Figure 2. The final parameters (intercept and slope) of the separating line were then determined with an iterative method. First, we adjusted the slope of the cut to maximize the bi-modality in Figure 2, and then we adjusted the intercept of the line to lie at the minimum between the two peaks. This method led to the following definition of a quiescent galaxy:

$$\begin{aligned} (U-V) &\geq 0.8(V-J) + 0.9; \\ (U-V) &> 1.33. \end{aligned} \tag{1}$$

This cut is in general agreement with the literature values, such as those reported by Williams et al. (2009) and Whitaker et al. (2015). Our cut is slightly higher, Williams et al. (2009) reports a slope of 0.88 and intercept of 0.69 while Whitaker et al. (2015) uses a slope of 0.8 and intercept of 0.7. These differences are likely due

[1] This cut is applied to remove possible contamination by blue star-forming galaxies.

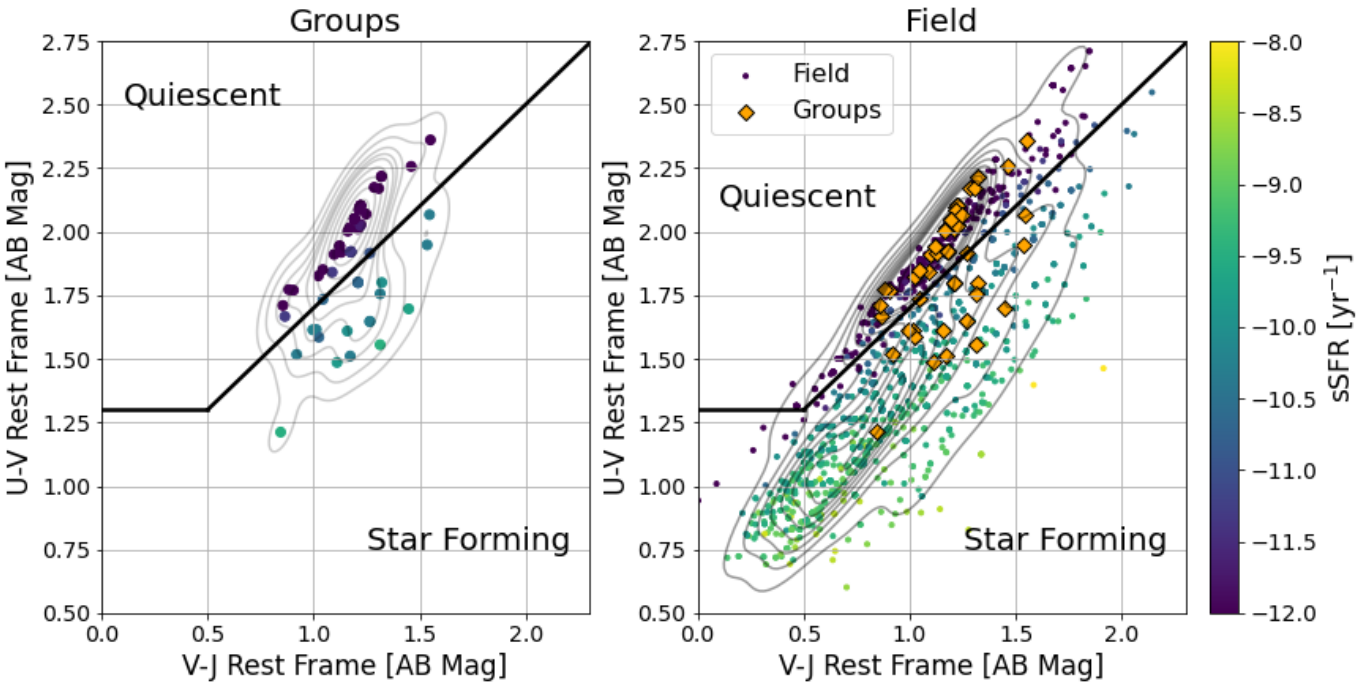

Figure 3. The UVJ diagram used to determine the quiescent and star-forming galaxies. The line indicates the cut used to separate quiescent and star-forming galaxies, details on how it was determined can be found in the text. The colors indicate the sSFR. In the left hand plot we have the group galaxies after the mass and luminosity cut. The right hand side are the field galaxies from the UVCANDELS COSMOS dataset that are above the $M_{cutoff} = 10.56$ mass cut, absolute $B-$band magnitude $M_B < -19.5 - 1.1z$ cut, and within the $0.2 \leq z < 0.8$ range. Overlaid on the right hand side are the group galaxies in orange diamonds. Contour lines are based on the density of points.

to differences in the bandpass definition used to compute the U-V, and V-J rest-frame colors in our analysis compared to others in the literature. Note that we do not consider a redshift-dependent selection of quiescent galaxies. Williams et al. (2009) find that the $U-V$ color for passive galaxies evolves by less than 0.15 magnitudes out to $z \sim 2$, and thus this effect is negligible in the redshift range considered here. The colors code of the points in Figure 3 confirms that in the selected region the majority of galaxies have low sSFR (sSFR< -11) associated with quenched objects, and we have found that our results remain the same if we instead classify quenched galaxies as those with an sSFR < -10.7 (Speagle et al. (2014); Jian et al. (2017)).

3.2. *The quenched fraction*

In this paper we investigate the probability of a galaxy being quenched, which we calculate in two ways. When calculating the probability of being quenched based off of a given parameter we use an MCMC logistic regression model. We use this logistic model to compute the probability of a galaxy being quenched based off of mass, redshift, and group-center distance. To do so we utilize the python module pymc3 with normal priors centered at 0 with a variance of 10. Using 1000 steps and the NUTS sampler we create models for each predictor. These models describe the probability of a massive galaxy being quenched, which we have defined as f_Q. This definition of f_Q is used in Figures 4, 5, and 6 to show how the probability of being quenching changes with redshift, group center distance, and galaxy mass.

In the sidebars of Figure 5 we define f_Q differently so we can get an estimate of f_Q averaged over the redshift bin, group centric radius, and mass. We follow the standard convention and define f_Q as the number of quenched galaxies (n_q) divided by the total number of galaxies (n_T) in that bin. To calculate the error on this version of f_Q we use Bayes theorem. We compute the posterior distribution on f_Q using Bayes theorem, assuming that the likelihood of observing n_Q quenched galaxies out of a sample of n_T is Binomial with probability f_Q of a galaxy being quenched. We use a Beta conjugate prior for f_Q, with parameters $\alpha = \beta = 1$. In each considered bin, we report the maximum a posteriori value of f_Q and the 68% credibility interval.

4. RESULTS

In Figure 4 we show the redshift evolution of the quenched fraction of galaxies more massive than $10^{10.56}$M$_\odot$ and with absolute $B-$band magnitude $M_B <$

$-19.5 - 1.1z$. We find that f_Q for group galaxies increases as redshift decreases, going from $0.66^{+0.11}_{-0.08}$ at $z = 0.8$ to $0.75^{+0.14}_{-0.08}$ at $z = 0.2$. For field galaxies our results suggest that the quenched fraction remains relatively constant as a function of redshift, with f_Q varying between $0.61^{+0.06}_{-0.06}$ to $0.62^{+0.08}_{-0.08}$. This result is in agreement with values reported in the literature (e.g., Knobel et al. (2013), Peng et al. (2010), Presotto et al. (2012), and Donnari et al. (2021)). For example, Presotto et al. (2012) find that the fraction of quenched galaxies among massive objects in groups increases from $0.8^{+0.03}_{-0.03}$ to $0.86^{+0.03}_{-0.03}$ between redshifts 0.65 and 0.3.

Figure 4 shows that the difference between field and group galaxies becomes stronger as redshift decreases. The overall trend of the group galaxies compared to the stagnant field suggests the group environment significantly influences a galaxy's probability of being quenched. This influence either occurs the longer a galaxy is in a group, or in groups that have formed at redshifts around 0.325. While the difference in f_Q between field and group galaxies does not differ by more than their standard deviations, the trend exhibited by the group galaxies suggests that the group environment is still influencing the evolution of galaxies in ways the field environment is not.

To investigate the timescale of environmental quenching within each redshift bin we explore the radial dependence of f_Q in Figure 5. In both panels we present the Bayesian estimate of f_Q, with both 68% and 95% credibility intervals, as a function of the normalized distance to the group center ($\Delta r/r_{gr}$). The left and right panels correspond to the redshift bins of $0.2 \leq z < 0.45$ and $0.45 \leq z < 0.8$, respectively. Blue circles in each panel show all galaxies, down to the mass limit indicated in the Figure, and included in the calculation of the probability. Finally, in each panel, we show the average values of f_Q for group and field galaxies.

Although the uncertainties are large, we see a clear radial dependence of f_Q in the lowest redshift bin. In the outskirt of groups, $f_Q = 0.4^{+0.25}_{-0.34}$, consistent with the average value measured in field galaxies ($f_Q = 0.57^{+0.06}_{-0.06}$). Moving toward the central parts of groups, f_Q increases smoothly, reaching values of $f_Q = 0.86^{+0.09}_{-0.11}$.

In comparison, the trend for the $0.45 \leq z < 0.8$ redshift range appears to be reversed, with the quenched probability increasing with distance from the group center. Here f_Q decreases from the outskirts of the groups ($f_Q = 0.87^{+0.10}_{-0.17}$) to the center of the groups ($f_Q = 0.61^{+0.15}_{-0.11}$). This is within agreement of the field values ($f_Q = 0.57^{+0.04}_{-0.04}$), and the relationship is statistically consistent with a flat distribution.

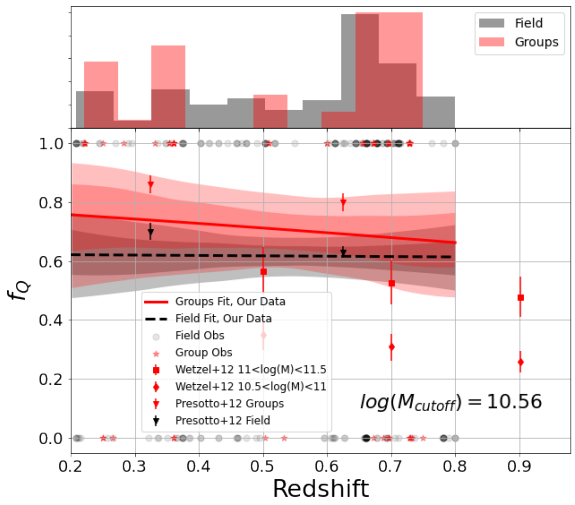

Figure 4. f_Q, which is defined as the probability of being quenched derived from a logistic regression model, plotted against the redshift of the group. Only galaxies with $M_B > -19.5 - 1.1 * z$ and $log(M/M_\odot) > 10.56$ were included. The red solid line corresponds to the logistic regression of the group galaxies, while the dashed black line corresponds to the logistic regression of the field galaxies.The shaded regions correspond to the 68% and 95% percentiles for each regression. The quenched and star-forming galaxies are plotted as 1 and 0, respectively. Field galaxies are denoted by the semi-transparent black circles, while the group galaxies are denoted by the red stars. Red squares and red diamonds indicate the field galaxies with $10.5 < logM < 11$ and $11 < logM < 11.5$ from Wetzel et al. (2013), respectively. Red upside-down triangles denote the field galaxies from Presotto et al. (2012), black upside-down triangles denote the group galaxies from Presotto et al. (2012).

To explore the possibility of these trends being driven by mass, in Figure 6 we investigate how the probability of being quenched changes with galaxy stellar mass. As in the previous figures, we show the logistic regression of f_Q and the corresponding 68% and 95% credibility intervals, with group galaxies in red and field galaxies in grey. The low and high redshift bins are shown on the left and right figures, respectively. The top panel in each figure, shows the mass distributions of galaxies in groups and the in the field.

In both redshift ranges considered, we find that the probability of being quenched depends in similar ways on the stellar mass for both group and field galaxies. Specifically, Figure 6 shows that f_Q increases with increasing mass, in groups and field in the two redshift

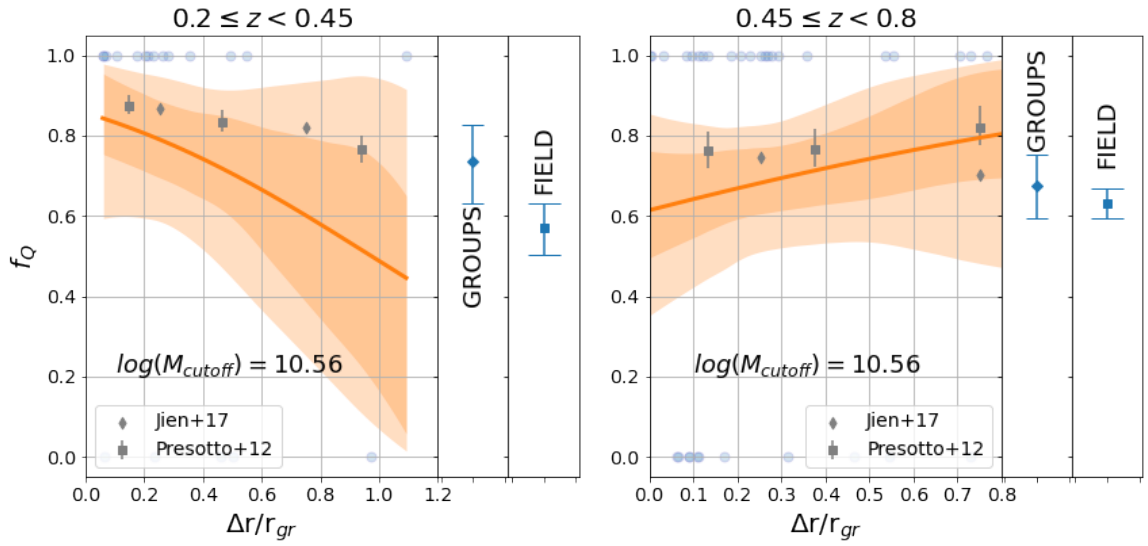

Figure 5. f_Q, which is defined as the probability of being quenched derived from a logistic regression model, plotted against the normalized distance to the group center. The points corresponding to quenched galaxies and star-forming galaxies are placed at 1 and 0, respectively. The left hand side is group galaxies within the $0.2 \leq z < 0.45$ range, the right hand plot is group galaxies within the $0.45 \leq z < 0.8$ range, both are limited to $log(M/M_{\odot}) \geq 10.56$ and $M_B < -19.5 - 1.1z$. The right hand sidebar of each plot indicates the total number of quenched galaxies, divided by the total number of galaxies, for each redshift bin in the groups and the field. The shaded regions correspond to the 68% and 95% intervals of the regression. Errorbars are derived by assuming a beta distribution prior to the binomial distribution that describes the quenched fraction. The errorbars are thus the standard deviation of the resulting beta-binomial distribution. Grey boxes denote the galaxies from Presotto et al. (2012), while the grey diamonds denote the galaxies from Jian et al. (2017).

intervals. These relationships are in relative agreement with the literature (Wetzel et al. (2013); Presotto et al. (2012)) with our values of f_Q being within the standard deviation of their results, with the overall trend remaining the same. Due to the mass dependence of f_Q the *radial* dependence of f_Q could be introduced if the mass distribution changes as a function of distance from the center of the group. We have tested this possibility and found that, at all redshifts, there is no correlation between a galaxy stellar mass and the distance to its group's center.

In Presotto et al. (2012) they studied the entire 20k zCOSMOS catalog, with similar mass, luminosity, and redshift cuts that we have placed on our data. The only difference between their cuts and ours is they place a lower mass and luminosity cut on the lower redshift bin, we maintain the same mass and luminosity cut for each redshift bin. While they did not focus on the dominant quenching process they did come to very similar trends in f_Q. The main differences are their values of f_Q are higher than ours, although still within 1 sigma of our results. If we adopt their definition of quiescence (based on a U-B vs Mass plot) then our results are closer to theirs, with the same trends we observe here.

We then because adopting the definition of quiescence change the value of f_Q we then verified if our method for determining quiescence was driving our results. There are a number of methods for determining if a galaxy is quiescent, U-B vs Mass plots, sSFR cuts, 4000Åbreak strengths, or UVJ plots to name a few. During our analysis we tried the sSFR method (with multiple different sSFR cuts), UVJ, and U-B vs Mass methods and found that the method does change the trends one obtains. While the method does change the value of f_Q it does not change how f_Q changes with We eventually went with UVJ as it involved the least amount of assumptions on the data, unlike sSFR or U-B vs Mass the UVJ plot takes the directly observed values, only using the redshift and colors to determine quiescence. Given a flat or positive slope is within the error of the trend we do not think that this is indicative of larger problems in the analysis. This is in agreement with simulations such as Donnari et al. (2021) where they show these differences in f_Q are present at masses logM ¿ 10.5, but the trends observed are roughly independent of the definition of quiescence.

5. DISCUSSION

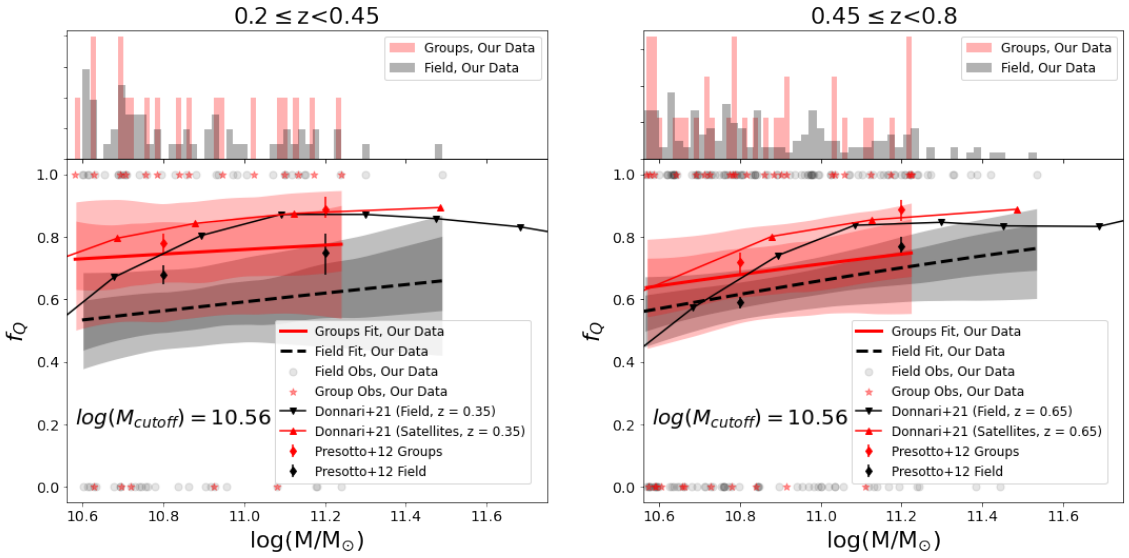

Figure 6. The bottom two plots indicate f_Q, which is defined as the probability of being quenched derived from a logistic regression model, plotted against the mass of the galaxies. The solid red line corresponds to the group galaxies, while the black dashed line corresponds to the field galaxies. The left hand side is group galaxies within the $0.2 \leq z < 0.45$ range, the right hand plot is group galaxies within the $0.45 \leq z < 0.8$ range, both are limited to $log(M/M_{\odot}) \geq 10.56$ and $M_B < -19.5 - 1.1z$. The shaded regions are the 68% and 95% percentiles from the regression models. Quenched galaxies and star-forming galaxies are plotted as 1 and 0, respectively. The group galaxies are plotted as red stars while the field galaxies are plotted as black circles. The top two plots are weighted histograms of the group and field mass distributions, weighted so the area under their histograms integrates to 1. Upside-down black triangles denote the simulation field values from Donnari et al. (2020), while the red triangles denote the simulated satellite galaxies from Donnari et al. (2020). The red diamons indicate the group values from Presotto et al. (2012), while the black diamonds denote the field values from Presotto et al. (2012).

In the previous section we have shown how the probability of being quenched (f_Q) for group galaxies depends on redshift, distance to the group center, and stellar mass. We have investigated these trends to assess what the most likely method for environmental quenching is in massive luminous galaxies in groups. As detailed in Section 1 environmental quenching processes can be broadly separated into rapid and slow processes depending on whether they remove the entirety of the cold material in a galaxy, or only act on the outermost, low-density gas.

Figure 4 presents the redshift evolution of f_Q for massive galaxies. This figure suggests that f_Q increases in massive galaxies in groups, as opposed to the trend observed in massive galaxies in the field, for which f_Q remains flat. While the overall trend of group galaxies shows a deviation from field galaxies, the trend itself doesn't exceed the standard deviation of the two populations in this range. This suggests that either galaxies are unlikely to quench due to the group environment, or the process itself takes Gyrs to cause a statistically significant difference between group and field galaxies. When observing this redshift trend we must keep in mind that as groups age they are likely accreting new members. That is, as the universe evolves from z = 0.8 new group members are accreted from the field and drive the value of f_Q in groups to mimic that of the field. If a rapid quenching method dominated in groups then this accretion would not significantly change f_Q over this range, as we are observing several Gyr and the rapid processes typically quench on the order of Myrs. Therefore, if we can assume that groups do cause significant quenching, Figure 4 suggests this quenching is dominated by a slow process for massive luminous galaxies in groups.

In order to better constrain whether the group environment increases the probability of quenching, we can look at the distribution of f_Q with how long specific galaxies have been in groups. To infer the latter, we can use the radial dependence of f_Q in groups. This follows from the assumption that the projected distance to the group center ($\Delta r/r_{gr}$) provides a measurement of the time since the galaxy's infall in the group halo. Numerical simulations confirm the validity of this assumption:

Taranu et al. (2014) show that out to approximately one and a half a cluster virial radius, the infall look-back time slowly declines with r, indicating that, statistically, galaxies projected closer to the center of groups have been in the group for longer. Therefore we look at Figure 5 which shows the relationship between f_Q and $\Delta r/r_{gr}$ for the two redshift bins that we have used. The lower redshift bin indicates that the closer a galaxy is to its group's center the more likely it is to be quenched. This indicates that the group environment does in fact influence the probability of being quenched, and combined with the results presented in Figure 4 suggests this process is dominated by slow environmental quenching.

The results presented are in contradiction with the higher redshift bin presented in Figure 5, where the longer a galaxy is in a group either does not change the probability of being quenched or this probability actually decreases. We believe that the differences between these two redshift bins can be partially accounted for by a combination of including non-virialized halos, the relationship between $\Delta r/r_{gr}$ and halo mass in this redshift bin, as well as preprocessing.

At higher redshifts projection effects in this case become less apparent, but the effects of contamination could be larger if the group halos themselves are not completely virialized. This means that the radius of the group is less well defined, and could be larger than the ones used. Halos are more likely to be virialized at lower redshifts, thus the effect of non-virialized group halos is more likely to be present in the higher redshift bin. We do expect these contributions to be minimized, as we limit our analysis to the purest group galaxy catalog. But, they would be more present in the higher redshift bin and could thus contribute to why the higher redshift bin disagrees with the lower redshift trend.

Another influence is from the relationship between halo mass and f_Q, which has been shown in observation and simulations to be related at low redshifts and low masses (Donnari et al. (2020), Wetzel et al. (2013)). Wetzel et al. (2013) shows that at z = 0.2 galaxies with masses $\log(M/M_\odot > 10.5$ f_Q is not dependent on the group halo mass. However Donnari et al. (2021) compared results from Jian et al. (2017),Lin et al. (2014), and Fossati et al. (2017) showing that f_Q is dependent on host halo mass at redshifts around z = 0.65. This study showed that at higher host halo masses f_Q is higher. Since the galaxies with low $\Delta r/r_{gr}$ in the high redshift bin predominantly belong to lower mass halos this could be driving the value of f_Q down in Figure 5 for the high redshift bin at low $\Delta r/r_{gr}$ while also driving f_Q up at high $\Delta r/r_{gr}$. Because group halo mass has been shown to not influence f_Q for our mass range at redshifts around 0.2 this effect will only be noticable in the higher redshift bin, partially accounting for the differences its trend.

Numerical simulations show that as we go down to a redshift of z $\sim$ 0 the probability that group members have spent time in other groups, known as preprocessed members, increases (Wetzel et al. (2013), Donnari et al. (2020), Sengupta et al. (2021)). This means that as we decrease in redshift the observed group members are more likely to have spent time in groups, while the groups at z $\sim$ 0.8 are more likely to be newly accreted members that have never been preprocessed. Given then that the galaxies in the higher redshift bin have spent less time in their groups than in the lower redshift bin we would expect them to still have a similar radial trend only if the dominant environmental process was rapid. Given that we do not see these similarities further suggests that galaxies must be in groups for billions of years in order to experience an increased probability of being quenched. Therefore, Figure 5 suggests the dominant environmental quenching process for massive galaxies in groups is slow.

While we have presented our arguments in support of a slow process for quenching we cannot firmly claim that these are the main processes involved in quenching in groups.

Uncertainty in the analysis discussed above could be introduced by the choice of the mock galaxy sample used to calibrate the group finding algorithms. For example, we present the results in terms of group-center projected distances normalized by the effective radius of the host halo. Donnari et al. (2021) demonstrated using numerical simulations that the slope of the trend is shallower when projected distances (instead of real 3D distances) are considered. A similar effect is likely introduced by contamination to the group sample by field galaxies.

Additionally, due to the coverage of the UVCANDELS dataset we are limited to the number of groups for which the rest-frame UV is directly probed, making our results subject to large uncertainties due to small-number statics. However, the relative good agreement we observe with the results of Presotto et al. (2012), who studied the full K12 sample) indicates that while a larger sample would decrease uncertainties, it would likely not drastically change the conclusions of this study.

In Jian et al. (2017), where they investigated groups in differing mass bins and found that the dominant process is more likely mergers. They do mention that a slow process is likely important, but due to their analysis in different mass bins they concluded that mergers were more likely the drivers of environmental quenching. With a larger sample we could mimic such analysis and see if

the UV data changes these conclusions. Furthermore with more data we could begin to probe the redshift relation with more accuracy. This could lead into an in depth analysis of preprocessing (Donnari et al. (2021); Wetzel et al. (2013); Taranu et al. (2014)). Or into the morphology of different galaxies, which has been suggested to highly influence the effects of environmental quenching (Li et al. (2020); Whitaker et al. (2015)).

Extrapolating our results to the halo masses of clusters gives us quenching values that are in relative agreement with the literature's (Wagner et al. (2016), Donnari et al. (2020)). These works show that in clusters quenching occurs to a larger percentage of observed and simulated galaxies. However the main mechanism does differ, in clusters the process of ram-pressure stripping is more effective and thus a fast process in clusters is more likely dominant in our mass and redshift range (Jian et al. (2017)). This is due to the larger galaxy number density and halo mass of clusters when compared to groups. But this shows that our results do follow the assumed evolution that groups will contribute to clusters, and thus f_Q in groups will be lower than cluster galaxies.

Comparing with clusters reveals a degeneracy in our data that we were unable to explore due to a low number of galaxies and groups. The mass of the host halo has been observed and simulated to affect the quenching process. The basic relationship is that with larger halo masses we have larger likelihoods of being quenching. This degeneracy could be influencing our data, and is a point we wish to explore when we combine this with the other field of UVCANDELS. This, among the previously mentioned unexplored variables, will be remedied by studies carried out on the upcoming Euclid Space Telescope data, allowing us to further contrain the main environmental quenching mechanisms in groups.

6. CONCLUSION

The evolution of a galaxy is driven, in part, by the environment that galaxy is in. Interactions with its environment can partially drive the cessation of star formation in that galaxy, known as quenching. The process of environmental quenching can be separated into two temporal categories, rapid and slow, which occur in millions or billions of years, respectively. Depending on the dominant process we expect differing redshift and radial trends in groups of galaxies.

To investigate the redshift and radial trends we take the 20k zCOSMOS catalog from Knobel et al. (2012) and calculate the physical properties of the galaxies using the UVCANDELS catalog data (Wang et al. in prep.). Using CIGALE SED fitting we are able to derive mass, SFR, and rest frame U-V and V-J colors of the galaxies. We take our sample of 20 groups and 53 galaxies that fit into our mass and luminosity complete sample and use an MCMC algorithm to determine how the probability of being quenched (defined as f_Q) changes with a galaxy's distance to its group center and group's redshift.

We found that f_Q is dependent on distance to the group's center and the group's redshift for our sample of massive luminous galaxies. f_Q changes slowly with redshift, from $0.67^{+0.10}_{-0.09}$ at 0.9 to $0.76^{+0.11}_{-0.13}$ at 0.2, compared to the field which remains stagnant around $0.62^{+0.08}_{-0.08}$ from z = 0.9 to 0.2, shown in Figure 4. Looking at the distribution of f_Q with group center distance in Figure 5 we find that f_Q is only clearly dependent on distance to group center in our lower redshift bin of $0.25 \leq z < 0.45$. While the further redshift bin is in disagreement to this we discuss why in Section 3. Combined with studies that show the statistical relationship between infall time and distance to the group's center these results tell us that environmental quenching is dominated by a slow quenching process.

To be sure that mass is not driving our conclusions we investigate the mass dependence of f_Q in Figure 6 and the radial dependence of mass. We find that, while f_Q is dependent on mass, there is no radial dependence of mass in our sample. This means that the radial dependence of f_Q is not being driven by the mass dependence of f_Q.

Therefore the relationship we see in Figure 5 is likely due to a slow quenching mechanism, such as strangulation (Larson et al. (1980)) or the delayed-then-rapid process (Wetzel et al. (2013)). The exact role of these methods over the others is not explored, and they could be marginally dominant over other environmental methods. It is clear though that galactic evolution for massive luminous galaxies is influenced by the group environment typically on the timescale of several billion years.

Our conclusions will be further investigated with the remaining three fields that were covered by the UVCANDELS survey. The UV data available in this survey allows us to further constrain the important role that groups have in quenching. We plan on utilizing these fields in future publications, and hopefully further constrain the exact timescale of the dominant environmental quenching process in groups.

Thanks to UVCANDELS here, need to know exactly what they want here.

Special thanks to Sean Bruton for his input and conversation on the topics discussed.

REFERENCES

Boquien, M., Burgarella, D., Roehlly, Y., et al. 2019, A&A, 622, A103, doi: 10.1051/0004-6361/201834156

Brammer, G. B., Whitaker, K. E., Dokkum, P. G. v., et al. 2011, The Astrophysical Journal, 739, 24, doi: 10.1088/0004-637X/739/1/24

Burgarella, D., Buat, V., & Iglesias-Páramo, J. 2005, MNRAS, 360, 1413, doi: 10.1111/j.1365-2966.2005.09131.x

Chabrier, G. 2003, Publications of the Astronomical Society of the Pacific, 115, 763, doi: 10.1086/376392

Chabrier, G. 2003, PASP, 115, 763, doi: 10.1086/376392

Charlot, S., & Fall, S. M. 2000, ApJ, 539, 718, doi: 10.1086/309250

Donnari, M., Pillepich, A., Nelson, D., et al. 2021, Monthly Notices of the Royal Astronomical Society, 506, 4760, doi: 10.1093/mnras/stab1950

Donnari, M., Pillepich, A., Joshi, G. D., et al. 2020, Monthly Notices of the Royal Astronomical Society, 500, 4004, doi: 10.1093/mnras/staa3006

Ford, A. B., Werk, J. K., Dave, R., et al. 2016, Monthly Notices of the Royal Astronomical Society, 459, 1745, doi: 10.1093/mnras/stw595

Fossati, M., Wilman, D. J., Mendel, J. T., et al. 2017, The Astrophysical Journal, 835, 153, doi: 10.3847/1538-4357/835/2/153

Gao, L., White, S. D. M., Jenkins, A., Stoehr, F., & Springel, V. 2004, Monthly Notices of the Royal Astronomical Society, 355, 819, doi: 10.1111/j.1365-2966.2004.08360.x

Gunn, J. E., & Gott, III, J. R. 1972, The Astrophysical Journal, 176, 1, doi: 10.1086/151605

He, Z., Wang, T., Liu, G., et al. 2019, Nature Astronomy, 3, 265, doi: 10.1038/s41550-018-0669-8

Iovino, A., Cucciati, O., Scodeggio, M., et al. 2010, Astronomy & Astrophysics, 509, A40, doi: 10.1051/0004-6361/200912558

Jeans, J. H., & Darwin, G. H. 1902, Philosophical Transactions of the Royal Society of London. Series A, Containing Papers of a Mathematical or Physical Character, 199, 1, doi: 10.1098/rsta.1902.0012

Jian, H.-Y., Lin, L., Lin, K.-Y., et al. 2017, The Astrophysical Journal, 845, 74, doi: 10.3847/1538-4357/aa7de2

Kawata, D., & Mulchaey, J. S. 2008, The Astrophysical Journal, 672, L103, doi: 10.1086/526544

Kitzbichler, M. G., & White, S. D. M. 2007, Monthly Notices of the Royal Astronomical Society, 376, 2, doi: 10.1111/j.1365-2966.2007.11458.x

Knobel, C., Lilly, S. J., Iovino, A., et al. 2009, The Astrophysical Journal, 697, 1842, doi: 10.1088/0004-637X/697/2/1842

—. 2012, The Astrophysical Journal, 753, 121, doi: 10.1088/0004-637X/753/2/121

Knobel, C., Lilly, S. J., Kovač, K., et al. 2013, The Astrophysical Journal, 769, 24, doi: 10.1088/0004-637X/769/1/24

Larson, R. B. 1972, Nature, 236, 21, doi: 10.1038/236021a0

Larson, R. B., Tinsley, B. M., & Caldwell, C. N. 1980, The Astrophysical Journal, 237, 692, doi: 10.1086/157917

Li, P., Wang, H., Mo, H. J., Wang, E., & Hong, H. 2020, The Astrophysical Journal, 902, 75, doi: 10.3847/1538-4357/abb66c

Lilly, S. J., Carollo, C. M., Pipino, A., Renzini, A., & Peng, Y. 2013, The Astrophysical Journal, 772, 119, doi: 10.1088/0004-637X/772/2/119

Lilly, S. J., Brun, V. L., Maier, C., et al. 2009, The Astrophysical Journal Supplement Series, 184, 218, doi: 10.1088/0067-0049/184/2/218

Lin, L., Jian, H.-Y., Foucaud, S., et al. 2014, The Astrophysical Journal, 782, 33, doi: 10.1088/0004-637X/782/1/33

Martig, M., Bournaud, F., Teyssier, R., & Dekel, A. 2009, The Astrophysical Journal, 707, 250, doi: 10.1088/0004-637X/707/1/250

Martis, N. S., Marchesini, D., Brammer, G. B., et al. 2016, The Astrophysical Journal, 827, L25, doi: 10.3847/2041-8205/827/2/L25

McPartland, C., Ebeling, H., Roediger, E., & Blumenthal, K. 2016, Monthly Notices of the Royal Astronomical Society, 455, 2994, doi: 10.1093/mnras/stv2508

Moore, B., Katz, N., Lake, G., Dressler, A., & Oemler, A. 1996, Nature, 379, 613, doi: 10.1038/379613a0

Murray, N., Ménard, B., & Thompson, T. A. 2011, The Astrophysical Journal, 735, 66, doi: 10.1088/0004-637X/735/1/66

Muzzin, A., Marchesini, D., Stefanon, M., et al. 2013, The Astrophysical Journal, 777, 18, doi: 10.1088/0004-637X/777/1/18

Nayyeri, H., Hemmati, S., Mobasher, B., et al. 2017, ApJS, 228, 7, doi: 10.3847/1538-4365/228/1/7

Noll, S., Burgarella, D., Giovannoli, E., et al. 2009, A&A, 507, 1793, doi: 10.1051/0004-6361/200912497

Oke, J. B. 1974, The Astrophysical Journal Supplement Series, 27, 21, doi: 10.1086/190287

Peng, Y.-j., Lilly, S. J., Kovač, K., et al. 2010, The Astrophysical Journal, 721, 193, doi: 10.1088/0004-637X/721/1/193

Presotto, V., Iovino, A., Scodeggio, M., et al. 2012, Astronomy & Astrophysics, 539, A55, doi: 10.1051/0004-6361/201118293

Sengupta, A., Keel, W. C., Morrison, G., et al. 2021, arXiv:2102.06612 [astro-ph]

Speagle, J. S., Steinhardt, C. L., Capak, P. L., & Silverman, J. D. 2014, The Astrophysical Journal Supplement Series, 214, 15, doi: 10.1088/0067-0049/214/2/15

Springel, V., White, S. D. M., Jenkins, A., et al. 2005, Nature, 435, 629, doi: 10.1038/nature03597

Taranu, D. S., Hudson, M. J., Balogh, M. L., et al. 2014, Monthly Notices of the Royal Astronomical Society, 440, 1934, doi: 10.1093/mnras/stu389

Wagner, C. R., Courteau, S., Brodwin, M., et al. 2016, The Astrophysical Journal, 834, 53, doi: 10.3847/1538-4357/834/1/53

Werk, J. K., Prochaska, J. X., Cantalupo, S., et al. 2016, The Astrophysical Journal, 833, 54, doi: 10.3847/1538-4357/833/1/54

Wetzel, A. R., Tinker, J. L., Conroy, C., & Bosch, F. C. v. d. 2013, Monthly Notices of the Royal Astronomical Society, 432, 336, doi: 10.1093/mnras/stt469

Whitaker, K. E., van Dokkum, P. G., Brammer, G., & Franx, M. 2012, The Astrophysical Journal, 754, L29, doi: 10.1088/2041-8205/754/2/L29

Whitaker, K. E., Franx, M., Bezanson, R., et al. 2015, The Astrophysical Journal, 811, L12, doi: 10.1088/2041-8205/811/1/L12

Williams, R. J., Quadri, R. F., Franx, M., van Dokkum, P., & Labbe, I. 2009, The Astrophysical Journal, 691, 1879, doi: 10.1088/0004-637X/691/2/1879

Zucca, E., Bardelli, S., Bolzonella, M., et al. 2009, Astronomy and Astrophysics, 508, 1217, doi: 10.1051/0004-6361/200912665